Green Chemistry

PAPER

View Article Online
View Journal | View Issue

Cite this: *Green Chem.*, 2020, **22**, 7823

Near neutral waterborne cationic polyurethane from CO_2-polyol, a compatible binder to aqueous conducting polyaniline for eco-friendly anti-corrosion purposes†

Chenyang Zou,[a,b] Hongming Zhang,[a] Lijun Qiao,[a] Xianhong Wang *[a,b] and Fosong Wang[a,b]

This work focuses on two meaningful points in green chemistry, one is providing a practical solution for CO_2 transformation into a CO_2 copolymer, and the other is disclosing the potential application of a CO_2 copolymer as a water dispersible binder to overcome the bottleneck in heavy metal free anti-corrosion coatings. For the first point, a CO_2-copolymer like CO_2-polyol is synthesized from the telomerization of CO_2 and propylene oxide using a zinc–cobalt double metal cyanide complex as a catalyst and terephthalic acid as a chain transfer agent. For the second point, for the past 30 years conducting polyaniline, with its unique anti-corrosion behaviour, has been regarded as a heavy metal free anti-corrosion material, but the development of a waterborne polyaniline anti-corrosion coating has encountered an impasse owing to the lack of a compatible binder. Therefore, a water borne cationic polyurethane dispersion (CPUD) was developed for this purpose, in which CO_2-polyol was used as a soft segment, and 1,4-butanediol di(3-diethylamino-2-hydroxypropyl alcohol) ether was synthesized as a side-chain cationic extender. Unlike earlier acidic water borne dispersions, this water borne CPUD was near neutral, ensuring good compatibility with an aqueous conducting polyaniline dispersion, and is expected to create significant possibilities for the development of a novel generation of sustainable and eco-friendly metal anti-corrosion materials.

Received 28th July 2020,
Accepted 5th October 2020

DOI: 10.1039/d0gc02592e

rsc.li/greenchem

Introduction

Recently, the efficient conversion of CO_2 into chemicals or synthetic fuels by using a suitable catalyst system has become a fascinating topic, driven by increased environmental loading due to CO_2 emission or the production of novel function materials.[1–6] One of these interesting activities is the synthesis of CO_2-polyol with a molecular weight in the oligomer range by the telomerization of CO_2 and propylene oxide (PO),[7,8] which is a potential sustainable feedstock in polyurethane (PU) manufacturing.[9] The design of catalysts for high activity and selectivity of CO_2-polyols has witnessed rapid development from bimetallic zinc complexes to salen-coordinated cobalt, chromium complexes, and aluminium complexes, and so on.[10–19] In 2016, Covestro achieved a 5000 t/a production line for CO_2-polyols in Dormagen, Germany.[20] Although the largest chemical utilization of CO_2 is for urea production,[21] the break-even cost per tonne of CO_2 for polyols is up to around −$2600, much larger than that of −$100 for urea, indicating that the pathway to polyols may be more profitable. Owing to the coexistence of carbonate and ether groups in the CO_2-polyol soft segment, the resulting polyurethanes exhibit specific hydrolysis and oxidation resistance in addition to affording suitable mechanical properties, which are a combination of polyester- and polyether-based polyurethanes.[22] However, the large commodity application of polyurethanes derived from CO_2-polyol is still difficult to achieve to date.

In another respect, metal corrosion is a worldwide topic because it not only causes substantial economic loss, but also results in security risks.[23–25] The state-of-the-art technique used to slow down metal corrosion is employing a zinc-rich coating or galvanized zinc sheet, a million ton scale application consuming a huge amount of zinc powder. In addition to affording a successful anti-corrosion performance, this technique is accompanied by heavy metal pollution and anxiety regarding the sustainable supply of exhausting zinc resources.[26,27] A possible alternative to mainstream zinc

[a]*Key Laboratory of Polymer Eco-materials, Changchun Institute of Applied Chemistry, Chinese Academy of Sciences, Changchun 130022, People's Republic of China. E-mail: xhwang@ciac.ac.cn; Fax: +86431 85689095; Tel: +86 431 85262250*
[b]*University of Science and Technology of China, Hefei, Anhui 230026, People's Republic of China*

†Electronic supplementary information (ESI) available: Synthesis details, spectroscopic characterization and thermal properties *etc*. See DOI: 10.1039/d0gc02592e

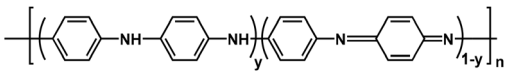

Scheme 1 Structure of polyaniline EB, in which *y* is between 0 and 1, and *n* is an integer.

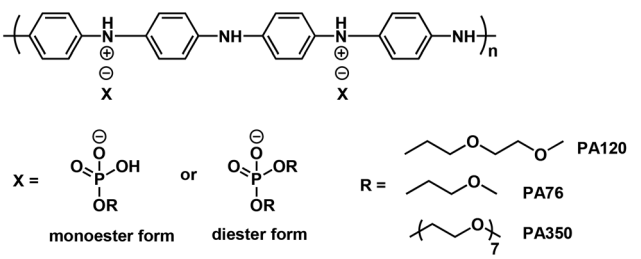

Scheme 2 Typical hydrophilic counter-anion induced water dispersible conducting polyaniline, in which X is a mixture of the monoester and diester phosphoric acid.

powder comes from polyaniline emeraldine base (EB), a synthetic polymer consisting of phenylenediamine and quinonediimine, the structure of which is shown in Scheme 1. Polyaniline has been regarded as an emerging environmentally friendly anti-corrosion material, as it displays anti-corrosion behaviour through its unique redox tunability, and therefore the anti-corrosion coating is heavy metal free.[28–30] However, the industrial application of a pure polyaniline coating in the anti-corrosion field is limited owing to its poor barrier performance to corrosive media such as water, oxygen or chloride ions, as well as its weak adhesion to metal.[31] To enhance the anti-corrosion performance of polyaniline, the designing of a coating containing polyaniline and a binder resin is a common sense strategy.

To date, most anti-corrosion polyaniline coatings that exhibit a good anti-corrosion performance are solvent based ones by virtue of the certain solubility of polyaniline in some organic solvents such as xylene or *N*-methylpyrrolidone.[17,32,33] To fulfil the waterborne processing of polyaniline for eco-friendly requirements, it is essential to prepare waterborne conducting polyaniline (cPANI), usually classified as water soluble or dispersible, which has been prepared since 1990.[34] However, most waterborne cPANI coatings afford a poor anti-corrosion behaviour, attributed to the lack of a suitable waterborne resin.[35–38]

Given the fact that water soluble cPANI displays a poor water resistance upon the formation of a coating, only water dispersible cPANI is able to fulfil the water resistant requirements. In the past two decades, significant progress has been made with regards to water dispersible cPANI. For example, highly conductive water dispersible conducting polyanilines (cPANIs) have been developed,[39] especially for polyaniline doped by PA76, an acidic phosphate with a hydrophilic ethylene oxide segment tail (Scheme 2, in which the R in the phosphate counter anion is monomethyl ethylene oxide), which possesses an electrical conductivity of 25 S cm^{-1} with a good water resistance upon film formation.[40] Therefore, cPANI again failed to form an effective anti-corrosion coating owing to the lack of a compatible binder.

As far as a waterborne binder resin is concerned, aqueous epoxy is the most often used resin for zinc rich coatings owing to its excellent barrier characteristics and its adhesion to the metal substrate, but it is not compatible with water borne conducting polyaniline. Waterborne polyurethane (WPU) is the next best to epoxy resin, it also displays an outstanding corrosion resistance, flexibility, strong adhesion to the metal substrates, and so on. However, only a few reports employ WPU as a binder to water borne conducting polyaniline for metal anti-corrosion purposes, and without exception they afford a poor anti-corrosion performance.[41]

Waterborne anionic polyurethane dispersions (APUDs) from CO_2-polyol have been developed using 2,2-dimethylol propionic acid as an internal emulsifier,[42,43] but they fail to act as compatible binders to PA76 doped polyaniline (cPANI), as their anionic nature leads to dedoping of cationic cPANI. Considering the cationic nature of cPANI, it would be logical to design a waterborne cationic polyurethane dispersion (CPUD). Generally, CPUD is prepared from an internal emulsifier with a tertiary amine, the ionic structure of the tertiary amine in the polyurethane backbone has a significant impact on the CPUD performance.[44] *N*-Methyl diethanolamine (MDEA) is therefore used to introduce the tertiary amine and to form a hydrophilic unit by a neutralization reaction with the acid.[45,46] It is well known that when the polymer is neutralized, the pH value of the dispersion is determined. If an equal molar amount of HOAc directly reacts with MDEA, all of the HOAc will be consumed giving a completely neutral solution. However, when MDEA is introduced into the polymer backbone, an incomplete neutralization reaction occurs as the tertiary amine group is enmeshed into the latex particle leading to an excess of the free acid.[44,47,48] It is noteworthy that the acidic resin is detrimental to the steel surface, let alone the anti-corrosion function. We attempted to use basic reagents (NaOH, Et_3N *etc.*) to neutralize the dispersion, but a precipitate appeared quickly, mainly because the hydrogen bonding that generally exists in CPUD was destroyed, which is relatively important to the stability of the dispersion. Therefore, in order to prepare a neutral or near-neutral CPUD for a specific anti-corrosion purpose, it is necessary to adjust the structure of the hydrophilic group to minimize the residual free acid as far as possible.

In this contribution, a near neutral CPUD was synthesized based on CO_2-polyol, in which a side-chain-type extender, 1,4-butanediol di(3-diethylamino-2-hydroxypropyl alcohol) ether (BDE), was designed and prepared. Compared to MDEA, the tertiary amine in BDE is located on the side chain with reduced steric hindrance, which is expected to consume more acid and is beneficial for producing neutral CPUD. The compatibility between the near neutral CPUD and cPANI dispersion was confirmed, producing a water borne composite

coating with an improved anti-corrosion performance. To demonstrate that CPUD with CO_2-polyol (PPC-diol for comparison with other polymer-diols), used as a soft segment, could provide a better anti-corrosion performance, CPUD from polytetramethylene ether glycol (PTMEG-diol) or polybutylene adipate glycol (PBA-diol) was also prepared for comparison.

Experimental

Chemicals

The following commercial reagents and solvents, isophorone diisocyanate (IPDI) (99%, J & K Scientific), dibutyltin dilaurate (DBTDL) (97.5%, J & K Scientific), 1,4-butanediol (BDO) (99%, J & K Scientific), acetic acid (HOAc) (99.8%, J & K Scientific), *N*-methyl diethanol amine (MDEA) (99%, Energy Chemical), 1,4-piperazinediethanol (PDE) (99%, Energy Chemical), 1,4-butanediol diglycidyl ether (93.0%, TCI), diethylamine (DEA) (99.5%, J & K Scientific), poly(tetrahydrofuran) diol (PTMEG-diol, with a number average molecular weight (M_n) of *Ca.* 2000 g mol^{-1}, Energy Chemical), polybutylene adipate glycol (PBA-diol, M_n of *Ca.* 2000 g mol^{-1}, Sinopharm), were used as received, unless otherwise noted.

Measurements

The molecular weight of CPUD was determined using gel permeation chromatography (GPC) at 35 °C on a Waters 410 GPC using a polystyrene standard with tetrahydrofuran (THF) as an eluent. The Fourier transform infrared spectroscopy (FT-IR) spectra were recorded on a Bruker TENSOR-27 spectrometer at a resolution of 4 cm^{-1} over a wavenumber range of 4000–500 cm^{-1}. The nuclear magnetic resonance (^{1}H NMR and ^{13}C NMR) spectra were obtained on a Bruker Avance-400 at room temperature using deuterated chloroform ($CDCl_3$) as a solvent. The particle size analysis of CPUD was carried out using dynamic laser scattering (DLS) using a QELS instrument with a vertically polarized He–Ne laser (DAWN EOS, Wyatt Technology).

The differential scanning calorimetric (DSC) curve was recorded on a PerkinElmer Thermal Analysis DSC-7 under nitrogen with a heating rate of 10 °C min^{-1}, and the thermogravimetric analysis (TGA) was performed on a Model TGA-7 system (PerkinElmer) in which the samples were heated from room temperature to 500 °C under a 20 mL min^{-1} nitrogen flow at a heating rate of 10 °C min^{-1}. A quadrupole ion mobility time-of-flight mass spectrometer equipped with an electrospray ionisation (ESI) source (Synapt G2S HDMS, Waters, Milford, MA, USA) was used for the mass spectrometry (MS) analysis, the following instrumental parameters were used in the positive mode: a cone voltage of 20 V, a capillary voltage of 2.2 kV, a source temperature of 80 °C, a desolvation temperature of 350 °C, cone gas flow of 30 L h^{-1}, desolvation gas of flow 500 L h^{-1}, and a nebulizer at 6.5 Bar. The high performance liquid chromatography (HPLC)-MS experiments were performed on a linear trap quadrupole (LTQ) ion trap mass spectrometer (Thermo, USA) in combination with an Accela liquid chromatography (LC) system having an Accela 1250 pump and an Accela autosampler.

The tensile stress–strain test was performed on an Instron-1121 at an extension rate of 100 mm min^{-1} at 25 °C, the films from the cationic polyurethane dispersions (CPUDs) were cut into a dumb-bell shape with a length of 20 mm and a width of 4 mm. The morphology of the composite coating was recorded on a FEI XL30 ESEM field emission scanning electron microscope (FESEM) at an operating voltage of 15 kV with a chromium coating, and the transmission electron microscopy (TEM) image was recorded on a JEOL JEM-2010 transmission electron microscope at an acceleration voltage of 200 kV.

To evaluate the barrier performance of the CPUD coating on carbon steel (CS), the CS plate was polished with fine abrasive paper, washed with deionized (DI) water, and consecutively sonicated in ethanol and acetone for 2 h each, CPUD was then cast onto the CS plate by dip-coating. The thickness of the CPUD coating was 75 ± 5 μm, as determined using a MiniTest 600 Electro Physik.

A potentiodynamic polarization (PDP) test was carried out by immersing the coated CS plate in 3.5 wt% NaCl solution at room temperature in a three-electrode glass cell consisting of a Ag/AgCl reference electrode, a platinum counter electrode, and a working electrode with an exposed area to corrosion media of 1.0 cm^2. The corrosion potential (E_{corr}) and corrosion current density (I_{corr}) values were evaluated by extrapolating their linear regions to the intersection point.[49] The polarization resistance (R_p) was determined from the Tafel plot using the Stearn–Geary equation. Electrochemical impedance spectroscopy (EIS) measurements were performed with a Solartron 1287 electrochemical interface and a Solartron 1255B Frequency Response Analyzer. The impedance data were collected at the open circuit potential with a 10 mV sinusoidal AC perturbation over a frequency range of 1000 kHz–0.01 Hz.

General procedure for preparation of the main chemicals and polymers

The PPC-diol (M_n = *Ca.* 2300 g mol^{-1}) with a carbonate unit content (CU%) of 56% was prepared by the telomerization of CO_2 and propylene oxide according to the method reported in our earlier work,[7] in which a zinc–cobalt double metal cyanide complex was used as a catalyst and terephthalic acid was used as a chain transfer agent.

BDE was synthesized using a modified procedure based on a previously reported method.[50] To a 250 ml single-neck round bottom flask with a magnetic stir bar was added 1,4-butanediol diglycidyl ether (16.18 g, 80 mmol), 28 g of diethylamine, and H_2O (30 ml), a yellow solution formed upon vigorous stirring at room temperature overnight. The reaction process was monitored using thin layer chromatograph (TLC), when the 1,4-butanediol diglycidyl ether had been completely consumed, another 30 ml of H_2O was added, after 10 min of stirring the mixture was extracted with diethyl ether three times (3 × 50 ml). The combined organic layer was dried over anhydrous Na_2SO_4, and the solvent was removed under reduced pressure to afford BDE. The chemical structure of BDE was

confirmed by ^{1}H-NMR and ^{13}C-NMR as well as MS analysis (Fig. S1–S3†). The purity of the BDE was found to be up to 98.3% as determined using HPLC-MS (Fig. S4†).

Polyaniline (EB) was prepared according to the method reported in our earlier publication,[40] its Mn was *Ca.* 22 500 g mol^{-1} with a polydispersity index (PDI) of 2.81. PA-76 was also prepared according to the method reported in the same publication.

The cPANI dispersion was prepared according to the method reported in our earlier publication,[39] in which 2.8 g of EB was mixed with 2.24 g of PA-76 in 500 ml of H_2O under vigorous stirring for 48 h at room temperature.

CPUD was prepared according to the route shown in Fig. 1, butanone was used as a solvent following the modified acetone method,[40] various CPUD samples with solid contents of *Ca.* 30.0 wt% were prepared. Taking PPC-BDE-4 as an example, to a three-necked round bottom flask equipped with a mechanical stirrer and a condenser, 5.0 g of butanone, 38.10 g of PPC-diol (CU% of 56%) and 16.76 g of IPDI were added under N_2 protection, and then 0.08 g of DBTDL was added as a catalyst, the reaction was carried out at 80 °C for 2 h. The reaction continued for another 6 h at 60 °C after 2.55 g of BDE was added in one portion, subsequently 4.57 g of BDO was added and the reaction was maintained at 60 °C for another 2 h, the endpoint of every step was monitored using the FT-IR technique. To neutralize the tertiary amine, 0.88 g of HOAc was added to produce the quaternary ammonium salts (QAS), and water was added dropwise with vigorous stirring after 30 min. The butanone was removed under reduced pressure at 40 °C to obtain CPUD. The synthetic protocols for the other CPUDs can be found in the ESI (Fig. S5–S9†). GPC traces and ^{1}H-NMR spectra of all the CPUDs are listed in the ESI (Fig. S10–S27†).

The composite dispersion of PPC-BDE-4(0.8) and cPANI was prepared by ball milling. Taking 1.0 wt% cPANI/CPUD as an example, their solid contents were determined in advance, for example 33.9% for PPC-BDE-4(0.8) and 24.7% for cPANI. At first, 0.358 g of cPANI was added to the PPC-BDE-4(0.8) dispersion with PPC-BDE-4(0.8) of 25.8 g, subsequently the mixture was ball milled for 7 h at 1200 rpm before it was filtered through the copper mesh.

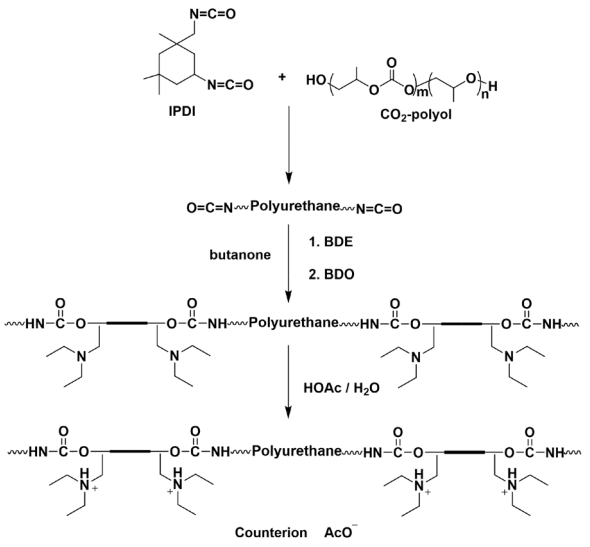

Fig. 1 Synthetic route to prepare PPC-BDE-4.

Results and discussion

Preparation of PPC-diol

According to the method reported in our earlier publication,[7] PPC-diol was prepared by the telomerization of CO_2 and PO using a zinc–cobalt double metal cyanide complex (Zn–Co-DMCC) as a catalyst and terephthalic acid as a chain transfer agent, the telomerization proceeded efficiently with a PO conversion above 95%. The chemical structure of PPC-diol was determined using ^{1}H NMR, as shown in Fig. S28,† in which the signals at 4.8–5.0 ppm and 3.9–4.3 ppm are characteristic of the CH and CH_2 groups in the carbonate segment, and those at 3.3–3.7 ppm represent the CH and CH_2 groups in the ether unit. The M_n and CU% of PPC-diol calculated using ^{1}H NMR were 2100 g mol^{-1} and 56%, respectively. Even though there was a difference, in that the M_n of PPC-diol was 2300 g mol^{-1}, obtained from GPC employing the polystyrene standard (Fig. S29†), the M_n of PPC-diol can be controlled conveniently by adjusting the molar ratio of PO and terephthalic acid.

Preparation of near neutral CPUDs

The structures of various oligomeric diols and chain extenders used in the preparation of CPUD are shown in Fig. 2, in which three oligomeric diols were chosen, including PPC-diol (CU% = 56%), PBA-diol and PTMG diol, and MDEA, PDE, and BDE were selected as chain extenders. As a main-chain type extender, the tertiary amine in PDE is confined inside the main-chain showing a rigid feature, and the methyl group attached to the N atom is flexible in MDEA,[46] whereas the tertiary amine in BDE is located on the side chain with a reduced steric hindrance, which is expected to be more reactive for neutralizing the acid and therefore beneficial for producing neutral CPUD. In addition, the thermal stability of the final polymer will be improved if BDE is used instead of MDEA or PDE, considering the difference in the bonding energy between C–N bond (305 kJ mol^{-1}) and C–C bond (346 kJ mol^{-1}).[51] As far as the oligomeric diols are concerned, PBA and CO_2-polyols are more rigid diols owing to the hard ester groups or carbonate groups,[9,43,52,53] although PTMEG is a soft oligomeric diol owing to its flexible ether segment.[54,55]

The hydrophilic group and hard segment contents from PPC-MDEA-4 to PTMEG-BDE-4 listed in Table 1 were controlled as 4 wt% and 40 wt%, respectively, while a 5 wt% hydrophilic group was used in PPC-PDE-5 for better stability. The neutralization degree was similar, that is, 100%, which was achieved by adding different molar equivalents of HOAc according to the number of N atoms per chain extender. In addition, their M_n values were adjusted with a difference

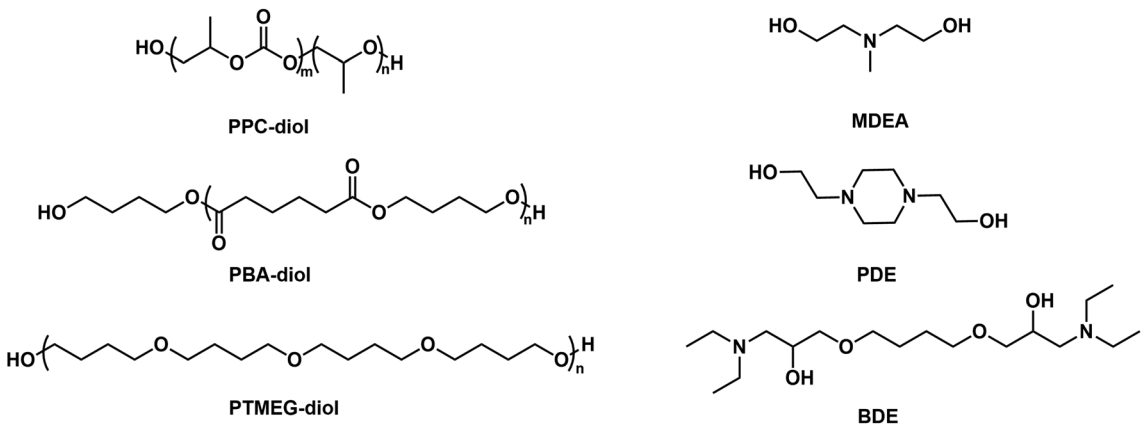

Fig. 2 Oligomeric diols and chain extenders used in the preparation of the CPUDs, from upper left to lower left these are PPC-diol, PBA-diol and PTMEG-diol, and from upper right to lower right these are MDEA, PDE and BDE, respectively.

Table 1 Preparation and basic characteristics of CPUDs using different chain extenders and polyols

Designation	N^+ content[a] (wt%)	Hydrophilic group[b] (wt%)	Hard segment (wt%)	Neutralization degree (mol. eq. HOAc)	Solid Content (wt%)	Particle size[c] (nm)	PDI[c]	Mn[d] (g mol^{-1})	pH[e]	Adhesion[f]
PPC-MDEA-4	0.47	4.0	40	1.0	32.4	200.4	0.16	24 390	4.15	4B
PPC-PDE-5	0.80	5.0	40	2.0	33.2	166.8	0.11	27 680	3.96	3B
PPC-BDE-4	0.32	4.0	40	2.0	32.9	180.1	0.18	26 750	4.69	5B
PBA-BDE-4	0.32	4.0	40	2.0	32.6	227.2	0.57	32 230	4.58	2B
PTMEG-BDE-4	0.32	4.0	40	2.0	34.1	193.6	0.27	31 880	4.54	1B
PPC-BDE-2	0.16	2.0	40	2.0	33.7	383.5	0.30	29 990	4.32	5B
PPC-BDE-6	0.48	6.0	40	2.0	32.8	83.4	0.32	30 860	5.20	5B
PPC-BDE-4(1)	0.16	4.0	40	1.0	34.2	225.5	0.12	27 680	5.41	5B
PPC-BDE-4(0.8)	0.13	4.0	40	0.8	33.9	306.6	0.10	34 910	5.67	5B

[a] N^+ content (wt%) refers to the cationic group content by weight. [b] The content of the hydrophilic group (wt%) calculated according to [(mass of CE)/(mass of IPDI + mass of BDO + mass of CE + mass of polyol)] × 100. [c] The particle size (nm) and PDI value were determined using DLS analyses. [d] The M_n (g mol^{-1}) value was determined using GPC analyses. [e] pH (water) = 6.23. [f] Test results were compared to ASTM D3359.

below 20%, that is, 27 680 ± 4550 g mol^{-1}. To evaluate the influence of the chain extenders and oligomeric polyols on the pH values, the solid content in CPUD was controlled as *Ca.* 30.0 wt% to eliminate the effect of the hydrogen ion concentration on pH. The whole preparation process was monitored using FT-IR technology (Fig. S30†), in which the complete disappearance of the peak at 2270 cm^{-1} from the NCO group was recorded. PPC-PDE-5 showed a particle size of 166.8 nm as its N^+ content reached 0.80 wt%, while PPC-BDE-4 with only 0.32 wt% N^+ content showed a particle size of 180.1 nm which was comparable to PPC-PDE-5, indicating that the tertiary amine located on the side chain can react with HOAc more efficiently. Correspondingly, PPC-BDE-4 exhibited a pH value of 4.69 even though 2.0 equivalents of HOAc were added, indicating that the CPUD using BDE as an internal emulsifier and PPC as soft segment had the potential to result in a neutral CUPD.

Therefore, as listed in Table 1, the CPUDs with different hydrophilic group contents and degrees of neutralization were prepared from PPC-diol and BDE. The pH value increased from 4.32 to 5.20 with an increase in the hydrophilic group content from 2.0 wt% to 6.0 wt%. Once the hydrophilic group content was controlled as 4.0 wt%, the pH value of CPUD increased from 4.69 to 5.67. As the pH value of water used was found to be 6.23, at least three near-neutral CPUDs were prepared, which were PPC-BDE-6, PPC-BDE-4(1) and PPC-BDE-4(0.8) with pH values of 5.20, 5.41 and 5.67, respectively.

As a binder resin for anti-corrosion purposes, in addition to the pH value, the water absorption rate of the dried coating is very important. As shown in Fig. S31,† the water absorption rate of PPC-BDE-6 reached 61.6% (72 h), which was attributed to the high content of exposed QAS, therefore it is not appropriate for use as a binder resin. In contrast, the water absorption rate for PPC-BDE-4(0.8) was only 4.73%, owing to its low QAS content of 0.13%, this CPUD is a potential binder resin thanks to the combination of the advantages of the near-neutral pH value and the low water absorption rate.

The thermal-mechanical properties of the CPUD coating are another important factor for the long-term metal anti-cor-

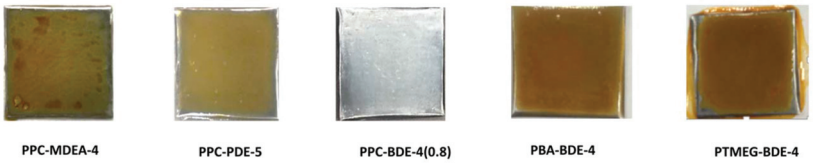

Fig. 3 Photographs of CS plates coated with PPC-MDEA-4 (far left), PPC-PDE-5 (left), PPC-BDE-4(0.8) (middle), PBA-BDE-4 (right) and PTMEG-BDE-4 (far right).

rosion purposes. The important thermal performance parameters of the CPUD films were obtained from TGA and are listed in Table S1,† in which T_5 refers to the temperature at which a 5% weight loss occurred. Owing to the more stable backbone, PPC-BDE-4 showed the highest T_5, T_{50} and T_{max} values compared with PPC-MDEA-4 and PPC-PDE-5. Meanwhile, with an increase in the BDE content from 2.0% to 6.0%, the glass transition temperature (T_g) of CPUD decreased from 5.16 °C to −0.06 °C (Fig. S36†), apparently the increasing side-chain structure of BDE in CPUD weakened the interchain interaction of the polymer.

The adhesion test between the CPUD coating and CS plate was performed according to the American Society for Testing and Materials (ASTM) D3359 standards,[56] in which the coating surface was divided into the same square lattices using a cross-cutter. As listed in Table 1, ASTM D3359 scale 5B level was achieved for the coating by using PPC-diol as a soft segment and a BDE internal emulsifier, in which no detachment of square lattices was observed, indicating the excellent adhesion of CPUD on the CS plate. It has been reported that tertiary amine groups can improve the adhesion strength of the binder.[57] Here, although all amine-containing monomers have tertiary amines, compared to MDEA and PDE, the tertiary amines in BDE are located on the side chain. When BDE was introduced to polyurethane, more tertiary amines are exposed on the surface of the polymer particle, making it easier to form contact with the CS plates, therefore affording a higher adhesion ability to the CS plates.

Anticorrosion performance of the pure CPUD resin

Fig. 3 shows photographs of the CS plates coated with PPC-MDEA-4, PPC-PDE-5 and PPC-BDE-4(0.8), respectively, the PPC-BDE-4(0.8) coated CS plate was visually transparent and as bright as a newly polished one, indicating the absence of flash rust owing to the near-neutral features of the dispersion. In contrast, light yellow was observed both in the other CPUD-coated CS plates, indicating the occurrence of corrosion on the steel surface attributed to the acidic micro-environment. The potentiodynamic polarization measurements of various CPUD coated CS plates were performed using a three-electrode cell after 3.0 h immersion in 3.5 wt% NaCl solution, the corresponding polarization curves are shown in Fig. 4, while the main kinetic parameters, including the corrosion current density (I_{corr}), corrosion potential (E_{corr}) and polarization resistance (R_p) are summarized in Table 2. The protection efficiency P_{EF} was calculated using the following equation:[58]

$$P_{EF}(\%) = \frac{I_{corr}(\text{bare steel}) - I_{corr}(\text{coated})}{I_{corr}(\text{bare steel})} \times 100\%$$

In which I_{corr}(bare steel) and I_{corr}(coated) are the corrosion current densities for bare steel and coated steel, respectively.

All the polarization curves exhibited a reasonably linear Tafel region in both the anodic and cathodic areas. The bare steel showed E_{corr} and I_{corr} values of −0.69 V and 36.5 μA cm^{-2}, respectively. The polarization resistance calculated for the bare steel was only 0.76 kΩ. Once it was coated with CPUD, all E_{corr} values were shifted to more positive values, accompanied by a significant decrease in the I_{corr}, indicating a certain anti-corrosion property of the resin. As higher E_{corr} or R_p values and a

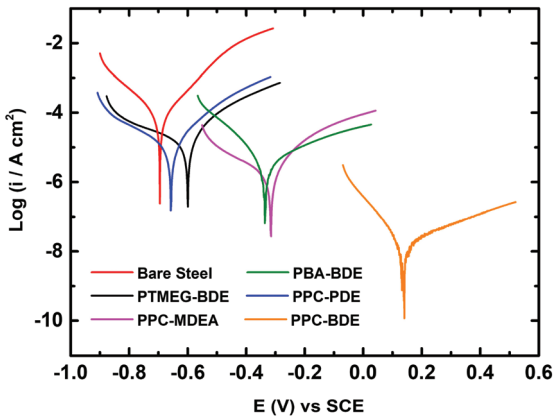

Fig. 4 PDP curves of bare steel and CPUDs-coated CS in 3.5 wt% NaCl solution for 3.0 h.

Table 2 Corrosion parameters obtained from the PDP studies for CPUDs-coated CS in 3.5 wt% NaCl solution

Designation	I_{corr} (μA cm^{-2})	E_{corr} (V)	R_p (kΩ)	P_{EF} (100%)
Bare steel	36.5	−0.69	0.76	0%
PPC-BDE-4(0.8)	0.02	0.14	824.2	99.9%
PPC-MDEA-4	2.51	−0.37	123.2	93.1%
PPC-PDE-5	14.1	−0.68	2.89	61.4%
PBA-BDE-4	4.71	−0.32	97.8	87.1%
PTMEG-BDE-4	20.0	−0.66	2.04	45.2%

lower I_{corr} value indicated a reduced corrosion rate and better corrosion protection,[59] the coatings using CPUD with CO_2-polyols as soft segments displayed a higher protection efficiency than those from PBA or PTMEG, these better barrier properties can be attributed to the presence of carbonate units. Another reason was a result of adhesion force, taking PBA-BDE-4 coated CS plate as example, although the initial P_{EF} reached up to 87.1%, the poor adhesion limited its further study. Among all the samples, the PPC-BDE-4(0.8) coated CS plate exhibited the best barrier properties, affording a low I_{corr} value of 0.02 μA cm^{-2} and a high E_{corr} value of 0.14 V, as well as a large enough R_p value of 824.2 kΩ. The P_{EF} value was up to 99.9% owing to the strong barrier property against O_2 and H_2O evidenced by the tight and parallel alignment inside this resin (Fig. S37†). However, for CS plates coated with PPC-MDEA-4 and PPC-PDE-5, the P_{EF} value was visibly lower than that of the PPC-BDE-4(0.8) coated CS plate, displaying more negative E_{corr} values of −0.37 and −0.68 V, and higher I_{corr} values of 2.51 and 14.1 μA cm^{-2}, respectively, which should be attributed to the acidic nature of the corresponding dispersion and the relatively weaker adhesion force. Therefore, the combination of a near neutral system and strong adhesion force to the CS plate for the PPC-BDE-4(0.8) coating contributed to the optimal corrosion protection performance, in which the former ensured the absence of flash rust before immersion in the corrosive solution, and the latter enabled long-term corrosion protection.

Anti-corrosion performance of the composite coating

Dispersion compatibility is a key factor to achieving uniform composite coatings. If the conducting polyaniline particles are not well dispersed in the polymer matrix, phase separation occurs forming agglomerates, leading to a poor anti-corrosion performance of the composite coating owing to increasing permeability to corrosive molecules. In contrast, a good dispersion compatibility between the cPANI dispersion and CPUD will increase the tortuosity of the diffusion path for corrosive molecules, leading to significantly enhanced barrier properties. Here PPC-BDE-4(0.8) was used as a waterborne binder resin for cPANI dispersion (1.0 wt% cPANI), the stability of the composite dispersion was evaluated by observing it in a transparent vial (Fig. 5a). No precipitate was found after it stood undisturbed at room temperature for 20 d. The cross sectional SEM image for the composite coating shown in Fig. 5b indicates that the fracture surface was flat and compact, again demonstrating the homogeneous dispersion of cPANI in the composite coating. Meanwhile, from the TEM image of the composite dispersion shown in Fig. 5c, a uniform distribution of the conducting polyaniline particles in PPC-BDE-4(0.8) was observed. In addition, the pH value of the composite dispersion is 5.61, a little lower than PPC-BDE-4(0.8), probably due to the presence of residual PA76 in cPANI. All of the above described features ensured the composite coating was able to serve the purposes of corrosion protection.

The anticorrosion performance of composite coating was evaluated using potentiodynamic polarization measurements and EIS. In addition to the above mentioned 1.0 wt% cPANI/CPUD, another three composite coatings containing 0.5 wt%, 2.0 wt% and 3.0 wt% of cPANI were prepared giving pH values of 5.65, 5.56 and 5.47, respectively. Their dispersion compatibility was also investigated. As shown in Fig. S38,† no precipitate or cPANI agglomerates were observed from the image of the 0.5 wt% cPANI/CPUD dispersion in a transparent vial, and the fracture surface was smooth, displaying a similar state to 1.0 wt% cPANI/CPUD. However, when the content of cPANI was increased, the surface became rough and even deformed (3.0 wt% cPANI) implying the presence of micropores, which can be verified by the potentiodynamic polarization measurements. As shown in Fig. 6a, the polarization curves showed a typical linear Tafel region in both the anodic and cathodic areas for the composite coatings. The I_{corr} of the cPANI/CPUD-coated CS plates with 1.0 wt% cPANI reached a minimum of 0.19 μA cm^{-2}, and the I_{corr} values of the composite coatings containing 0.5 wt% cPANI or 3.0 wt% cPANI were found to be 0.74 or 4.57 μA cm^{-2}, obviously higher than that of the 1.0 wt% cPANI composite coating. Moreover, the corrosion potential of the cPANI/CPUD-coated CS plates with 1.0 wt% cPANI was −0.02 V, which was more positive than the composite coatings containing 0.5 wt% cPANI or 3.0 wt% cPANI, the corrosion potential of which was found to be −0.17 or −0.28 V. Compared to the pure CPUD resin with an I_{corr} of 2.95 μA cm^{-2}, the 3.0 wt% cPANI/CPUD coating exhibited a larger I_{corr}, implying that the cPANI agglomerate existed, weakening the tortuosity of the diffusion path for corrosive molecules. The composite coating containing 1.0 wt% cPANI showed an optimal corrosion protection performance, indicating that the

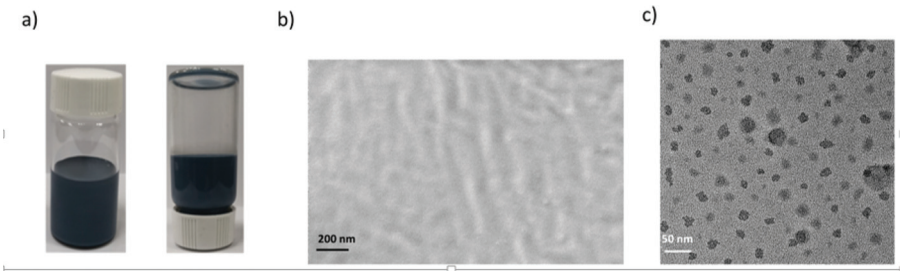

Fig. 5 (a) Photograph of the composite dispersion in a transparent vial after standing for 20 d; (b) cross section SEM image of the fracture surface for the composite coating; and (c) TEM image of the composite dispersion.

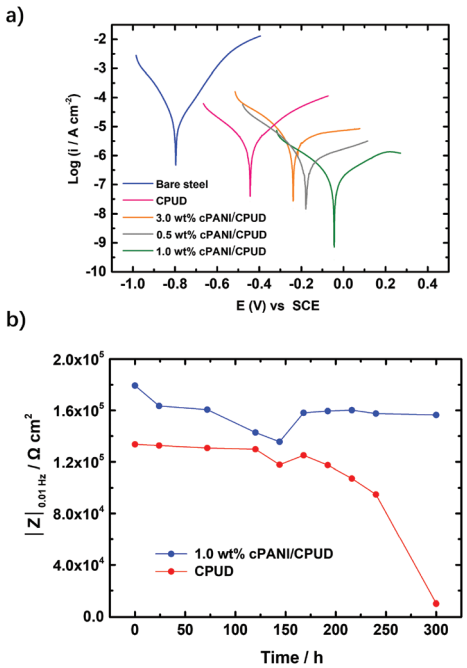

Fig. 6 (a) PDP curves for bare steel, pure CPUD and composite coatings in 3.5 wt% NaCl solution; and (b) plots of $|Z|_{0.01\ Hz}$ against the immersion time for pure CPUD and the 1.0 wt% cPANI/CPUD composite coating.

cPANI loading in composite coating should be kept low to ensure constituent compatibility.

According to the previously reported literature,[37,60] the impedance modulus at 0.01 Hz ($|Z|_{0.01\ Hz}$) is an important parameter for evaluating the anticorrosion properties of coatings. Therefore, the plots of $|Z|_{0.01\ Hz}$ against immersion time for pure resin and composite coating containing 1.0 wt% cPANI are shown in Fig. 6b. The initial $|Z|_{0.01\ Hz}$ of the pure resin was 1.34×10^5 Ω cm^2, whereas that of the composite coating was 1.80×10^5 Ω cm^2. Although only a slight increase of *Ca.* 20% was realized for the composite coating containing 1.0% cPANI, the $|Z|_{0.01\ Hz}$ of pure resin dropped slowly before 170 h immersion, but it experienced a rapid decrease later, suggesting the coating became porous and the corrosion medium gradually arrived at the surface of the substrate leading to the occurrence of corrosion. However, for the composite coating with the 1.0 wt% cPANI protected CS plate, the $|Z|_{0.01\ Hz}$ dropped to 1.36×10^5 Ω cm^2 at 145 h, and then increased to a plateau of 1.59×10^5 Ω cm^2, which was attributed to the passivation of the CS surface by cPANI. Although the $|Z|_{0.01\ Hz}$ of the composite coating containing 1.0 wt% of cPANI was under 10^6 Ω cm^2, which was attributed to the linear internal structure of PPC-BDE-4(0.8), lower than that reported for the waterborne anti-corrosion coatings containing cPANI using a waterborne epoxy resin as a binder,[35,37] the two obstacles including the incompatibility between the cPANI and binder and the inherent acidity of the binder were solved by using the PPC-BDE-4(0.8) resin. In the future, an internally crosslinked dispersion should be constructed based on this investigation to achieve a better barrier performance. Concerning the alkaline crosslinking agent, for example trimethylolpropane-tris-(β-*N*-aziridinyl) propionate that will destroy the stability of dispersion, a neutral or acidic crosslinking agent such as 1,2,3-tribromopropane or citric acid may be a suitable choice.[61]

Conclusions

Using CO_2-polyol(PPC-diol) as a soft segment and BDE as a side-chain-cationic internal emulsifier, the tertiary amine of which is located on the side chain with minimal steric hindrance, CPUD (PPC-BDE-4(0.8)) with a pH value of 5.67 was prepared. The CPUD was compatible with a water borne cPANI dispersion. A typical composite dispersion (PPC-BDE-4(0.8) + 1.0 wt% PANI-PA76) showed a good stability and compatibility for efficient corrosion protection, and the successful incorporation of cPANI into the CPUD composite coating afforded a significant enhancement in the barrier properties and passivation behaviour, as evidenced by the PDP and EIS analyses. These results indicate that the near neutral water borne binder from CO_2-polyol has great potential for use in anticorrosion applications.

Conflicts of interest

There are no conflicts to declare.

Acknowledgements

Financial support from the National Natural Science Foundation of China (Basic Science Center Program, Gr. No. 51988102) is greatly appreciated.

Notes and references

1 M. Aresta, A. Dibenedetto and A. Angelini, *Chem. Rev.*, 2014, **114**, 1709–1742.
2 J. Klankermayer and W. Leitner, *Science*, 2015, **350**, 629–630.
3 J. Artz, T. E. Müller, K. Thenert, J. Kleinekorte, R. Meys, A. Sternberg, A. Bardow and W. Leitner, *Chem. Rev.*, 2018, **118**, 434–504.
4 P. Markewitz, W. Kuckshinrichs, W. Leitner, J. Linssen, P. Zapp, R. Bongartz, A. Schreiber and T. E. Müller, *Energy Environ. Sci.*, 2012, **5**, 7281–7305.
5 C. Hepburn, E. Adlen, J. Beddington, E. A. Carter, S. Fuss, N. Mac Dowell, J. C. Minx, P. Smith and C. K. Williams, *Nature*, 2019, **575**, 87–97.
6 Y. Zhu, C. Romain and C. K. Williams, *Nature*, 2016, **540**, 354–362.
7 Y. Gao, L. Gu, Y. Qin, X. Wang and F. Wang, *J. Polym. Sci., Part A: Polym. Chem.*, 2012, **50**, 5177–5184.

8 S. Fu, Y. Qin, L. Qiao, X. Wang and F. Wang, *Acta Polym. Sin.*, 2019, **50**, 338–343.
9 J. Langanke, A. Wolf, J. Hofmann, K. Böhm, M. A. Subhani, T. E. Müller, W. Leitner and C. Gürtler, *Green Chem.*, 2014, **16**, 1865–1870.
10 G.-P. Wu, S.-H. Wei, W.-M. Ren, X.-B. Lu, B. Li, Y.-P. Zu and D. J. Darensbourg, *Energy Environ. Sci.*, 2011, **4**, 5084–5092.
11 M. W. Lehenmeier, S. Kissling, P. T. Altenbuchner, C. Bruckmeier, P. Deglmann, A.-K. Brym and B. Rieger, *Angew. Chem., Int. Ed.*, 2013, **52**, 9821–9826.
12 H. Cao, Y. Qin, C. Zhuo, X. Wang and F. Wang, *ACS Catal.*, 2019, **9**, 8669–8676.
13 S. Elmas, M. A. Subhani, M. Harrer, W. Leitner, J. Sundermeyer and T. E. Müller, *Catal. Sci. Technol.*, 2014, **4**, 1652–1657.
14 S. Elmas, M. A. Subhani, H. Vogt, W. Leitner and T. E. Müller, *Green Chem.*, 2013, **15**, 1356–1360.
15 Y. Liu, W.-M. Ren, J. Liu and X.-B. Lu, *Angew. Chem., Int. Ed.*, 2013, **52**, 11594–11598.
16 X.-B. Lu, *Nat. Chem.*, 2020, **12**, 324–326.
17 Y. Liu, L.-M. Fang, B.-H. Ren and X.-B. Lu, *Macromolecules*, 2020, **53**, 2912–2918.
18 A. C. Deacy, A. F. R. Kilpatrick, A. Regoutz and C. K. Williams, *Nat. Chem.*, 2020, **12**, 372–380.
19 G. S. Sulley, G. L. Gregory, T. T. D. Chen, L. Peña Carrodeguas, G. Trott, A. Santmarti, K.-Y. Lee, N. J. Terrill and C. K. Williams, *J. Am. Chem. Soc.*, 2020, **142**, 4367–4378.
20 A. Scott, *Chem. Eng. News*, 2015, **93**, 10–16.
21 S. M. Jarvis and S. Samsatli, *Renewable Sustainable Energy Rev.*, 2018, **85**, 46–68.
22 Z. Ma, X. Zhang, X. Zhang, N. Ahmed, H. Fan, J. Wan, C. Bittencourt and B.-G. Li, *Ind. Eng. Chem. Res.*, 2020, **59**, 3044–3051.
23 R. C. Newman and K. Sieradzki, *Science*, 1994, **263**, 1708–1709.
24 D. E. Tallman, G. Spinks, A. Dominis and G. G. Wallace, *J. Solid State Electrochem.*, 2002, **6**, 73–84.
25 F. Zhang, L. Zhao, H. Chen, S. Xu, D. G. Evans and X. Duan, *Angew. Chem., Int. Ed.*, 2008, **47**, 2466–2469.
26 H. Liu, S. Szunerits, W. Xu and R. Boukherroub, *ACS Appl. Mater. Interfaces*, 2009, **1**, 1150–1153.
27 S. Shreepathi, P. Bajaj and B. P. Mallik, *Electrochim. Acta*, 2010, **55**, 5129–5134.
28 D. W. DeBerry, *J. Electrochem. Soc.*, 1985, **132**, 1022.
29 B. Wessling, *Adv. Mater.*, 1994, **6**, 226–228.
30 A. Vimalanandan, L.-P. Lv, T. H. Tran, K. Landfester, D. Crespy and M. Rohwerder, *Adv. Mater.*, 2013, **25**, 6980–6984.
31 J. R. Santos, L. H. C. Mattoso and A. J. Motheo, *Electrochim. Acta*, 1998, **43**, 309–313.
32 Y. Chen, X. H. Wang, J. Li, J. L. Lu and F. S. Wang, *Corros. Sci.*, 2007, **49**, 3052–3063.
33 Y. Zhang, Y. Shao, T. Zhang, G. Meng and F. Wang, *Corros. Sci.*, 2011, **53**, 3747–3755.
34 J. Yue and A. J. Epstein, *J. Am. Chem. Soc.*, 1990, **112**, 2800–2801.
35 F. Chen and P. Liu, *ACS Appl. Mater. Interfaces*, 2011, **3**, 2694–2702.
36 J. A. Syed, S. Tang, H. Lu and X. Meng, *Ind. Eng. Chem. Res.*, 2015, **54**, 2950–2959.
37 S. Qiu, C. Chen, M. Cui, W. Li, H. Zhao and L. Wang, *Appl. Surf. Sci.*, 2017, **407**, 213–222.
38 Z. Tian, H. Yu, L. Wang, M. Saleem, F. Ren, P. Ren, Y. Chen, R. Sun, Y. Sun and L. Huang, *RSC Adv.*, 2014, **4**, 28195–28208.
39 J. Luo, H. Zhang, X. Wang, J. Li and F. Wang, *Macromolecules*, 2007, **40**, 8132–8135.
40 H. Zhang, J. Lu, X. Wang, J. Li and F. Wang, *Polymer*, 2011, **52**, 3059–3064.
41 K. Cai, S. Zuo, S. Luo, C. Yao, W. Liu, J. Ma, H. Mao and Z. Li, *RSC Adv.*, 2016, **6**, 95965–95972.
42 J. Wang, H. Zhang, Y. Miao, L. Qiao and X. Wang, *Green Chem.*, 2017, **19**, 2194–2200.
43 J. Wang, H. Zhang, Y. Miao, L. Qiao, X. Wang and F. Wang, *Green Chem.*, 2016, **18**, 524–530.
44 A. K. Nanda and D. A. Wicks, *Polymer*, 2006, **47**, 1805–1811.
45 Y. Lu and R. C. Larock, *ChemSusChem*, 2010, **3**, 329–333.
46 Y. Xia, Z. Zhang, M. R. Kessler, B. Brehm-Stecher and R. C. Larock, *ChemSusChem*, 2012, **5**, 2221–2227.
47 A. K. Nanda, D. A. Wicks, S. A. Madbouly and J. U. Otaigbe, *J. Appl. Polym. Sci.*, 2005, **98**, 2514–2520.
48 X. Z. Kong, X. Zhu, X. Jiang and X. Li, *Polymer*, 2009, **50**, 4220–4227.
49 G. S. Frankel, in *Fundamentals of Corrosion Kinetics, in Active Protective Coatings: New-Generation Coatings for Metals*, ed. A. E. Hughes, J. M. C. Mol, M. L. Zheludkevich and R. G. Buchheit, Springer Netherlands, Dordrecht, 2016, pp. 17–32.
50 N. Azizi and M. R. Saidi, *Org. Lett.*, 2005, **7**, 3649–3651.
51 T. L. Cottrell, *The Strengths of Chemical Bonds*, Butterworths Scientific Publications, 1958.
52 M. A. Subhani, B. Köhler, C. Gürtler, W. Leitner and T. E. Müller, *Angew. Chem., Int. Ed.*, 2016, **55**, 5591–5596.
53 M. Pohl, E. Danieli, M. Leven, W. Leitner, B. Blümich and T. E. Müller, *Macromolecules*, 2016, **49**, 8995–9003.
54 P. Alagi, R. Ghorpade, Y. J. Choi, U. Patil, I. Kim, J. H. Baik and S. C. Hong, *ACS Sustainable Chem. Eng.*, 2017, **5**, 3871–3881.
55 K. Kojio, T. Fukumaru and M. Furukawa, *Macromolecules*, 2004, **37**, 3287–3291.
56 T. Balakrishnan, S. Sathiyanarayanan and S. Mayavan, *ACS Appl. Mater. Interfaces*, 2015, **7**, 19781–19788.
57 T.-W. Chuo and Y.-L. Liu, *Polymer*, 2017, **125**, 227–233.
58 C.-J. Weng, C.-H. Chang, C.-W. Peng, S.-W. Chen, J.-M. Yeh, C.-L. Hsu and Y. Wei, *Chem. Mater.*, 2011, **23**, 2075–2083.
59 H. Wei, D. Ding, S. Wei and Z. Guo, *J. Mater. Chem. A*, 2013, **1**, 10805–10813.
60 J. H. Park, G. D. Lee, A. Nishikata and T. Tsuru, *Corros. Sci.*, 2002, **44**, 1087–1095.
61 A. Bossion, I. Olazabal, R. H. Aguirresarobe, S. Marina, J. Martín, L. Irusta, D. Taton and H. Sardon, *Polym. Chem.*, 2019, **10**, 2723–2733.